Hydrol. Earth Syst. Sci. Discuss., 10, 5355–5395, 2013
www.hydrol-earth-syst-sci-discuss.net/10/5355/2013/
doi:10.5194/hessd-10-5355-2013

Hydrology and Earth System Sciences
Open Access
Discussions

Regional GRACE-based estimates of water mass variations over Australia: validation and interpretation

L. Seoane[1], **G. Ramillien**[1], **F. Frappart**[1], **and M. Leblanc**[2]

[1]Géosciences Environnement Toulouse GET – UMR5563, CNRS, Université de Toulouse UPS, GRGS, 14, Avenue E. Belin, 31400 Toulouse, France
[2]School of Earth & Environmental Sciences, James Cook University, Cairns, 4878, QLD, Australia

Received: 13 March 2013 – Accepted: 5 April 2013 – Published: 29 April 2013

Correspondence to: L. Seoane (lucia.seoane@get.obs-mip.fr)

Published by Copernicus Publications on behalf of the European Geosciences Union.

Abstract

Time series of regional 2°-by-2° GRACE solutions have been computed from 2003 to 2011 with a 10 day resolution by using an energy integral method over Australia [112° E 156° E; 44° S 10° S]. This approach uses the dynamical orbit analysis of GRACE Level 1 measurements, and specially accurate along-track K Band Range Rate (KBRR) residuals (1 μm s^{-1} level of error) to estimate the total water mass over continental regions. The advantages of regional solutions are a significant reduction of GRACE aliasing errors (i.e. north–south stripes) providing a more accurate estimation of water mass balance for hydrological applications. In this paper, the validation of these regional solutions over Australia is presented as well as their ability to describe water mass change as a reponse of climate forcings such as El Niño. Principal component analysis of GRACE-derived total water storage maps show spatial and temporal patterns that are consistent with independent datasets (e.g. rainfall, climate index and in-situ observations). Regional TWS show higher spatial correlations with in-situ water table measurements over Murray–Darling drainage basin (80–90 %), and they offer a better localization of hydrological structures than classical GRACE global solutions (i.e. Level 2 GRGS products and 400 km ICA solutions as a linear combination of GFZ, CSR and JPL GRACE solutions).

1 Introduction

The Gravity Recovery and Climate Experiment (GRACE) space gravity mission, launched in 2002, provides for the first time global estimates of changes in total water storage (surface water, soil moisture and groundwater) with unprecedented accuracy at global scales. GRACE data have already demostrated a strong potential for estiming hydrological information such as discharges (Syed et al., 2008), evapotranspiration (Rodell et al., 2004; Ramillien et al., 2006a), groundwater (Rodell et al., 2007; Leblanc et al., 2009) and extreme climate events as floods and droughts (Andersen et al., 2005;

HESSD
10, 5355–5395, 2013

Frappart et al., 2012, 2013; Houborg et al., 2012). Several analysis centres, including the Centre for Space Research, University of Texas at Austin (CSR), Jet Propulsion Laboratory (JPL), GeoForschungsZentrum (GFZ) and Groupe de Recherche en Géodésie Spatiale (GRGS), use GRACE Level 1B observations to produce time series of global gravity solutions in terms of spherical harmonics. However, this type of representation of the Earth's gravity field remains limited by errors with a north–south striping pattern that degrades accuracy of the solutions, the effect of aliasing and the influence of signals coming from regions outside the target basin. Filtering techniques can partly remove some of these effects (Swenson et al., 2006; Klees et al., 2008; Frappart et al., 2011). New regional GRACE solutions using an energy integral method (Ramillien et al., 2011, 2012) yield to significant gains in the accuracy and resolution of total water storage estimates compared to those using the classical spherical harmonic approach. The present study aims to test these new regional solutions over the Australian continent; the driest inhabited continent. In average the seasonal amplitude of TWS in Australia is 3 times lower than that observed in the Amazon. The challenge is to detect realistic structures while noise amplitude in GRACE data is closer to the amplitude of the true water mass variations over the continent. Water storage variations from regional solutions over Australia are validated with independent information given by the in-situ observations (rainfall, groundwater levels). GRACE products have already been used to study time variations of water mass storages and transfers over Australia. Syed et al. (2008) used GRACE data to estimate a depletion of 1.3 mm month^{-1} of total water storage in Australia. Leblanc et al. (2009) used GRACE global solutions to analyze the impact of the Millennium drought on the water resources in the Murray–Darling Basin. Awange et al. (2009) noted the relatively small hydrological signal typical for much of Australia were not detectabled because of errors int the standard GRACE data processing (e.g. oceanic non-tidal model deficiencies) and filtering methods. Tregoning et al. (2008) showed the propagation of error of non-tidal oceanic modelling in the Gulf of Carpentaria onto the continent in northern Queensland and the Northern Territory. Frappart et al. (2011) proposed a filtering technique based on Independent Component

HESSD
10, 5355–5395, 2013

Analysis that better reproduced the in situ observations over the Murray–Darling Basin than the spherical harmonic solutions obtained using other filtering.

Our regional approach using the energy integral method can potentially further improve the accuracy of GRACE TWS estimations. Over South America, Ramillien et al. (2012) have shown that thos regional approach offers a reduction of north–south striping due to mission configuration and temporal aliasing.

The present study aims to test these new regional solution over the Australian continent. The challenge is to detect realistic structures while noise amplitude in GRACE data is closer to the amplitude of the true water mass variations over the continent.

In the next section, all the datasets used are presented. Then, we discuss the results of the Principal Component Analaysis (PCA) separation in space and time modes of GRACE TWS solutions in the third section. We interpret each of them in the terms of individual hydrological structrures by the distinction of ground and surface water systems and empirical climatic indexes. Analysis of GRACE signals over Australia using PCA have already been proposed in previous studies (Reiser et al., 2010; García-García et al., 2011; Awange et al., 2011; Forootan and Kusche, 2012). For further validation, we compared the new regional solutions to three in-situ and modelled hydrologic datasets: (1) rainfall across the continent; (2) surface and subsurface strorage in the Murray–Darling Basin; (3) streamflow data in the Fitzroy Basin (see Fig. 1). The conclusion of our analysis is given in Sect. 4.

2 Datasets

2.1 GRACE land waters products

2.1.1 Regional solutions

An alternative regional approach to the classical global one has been recently proposed to improve geographical localization of hydrological structures and to reduce

HESSD
10, 5355–5395, 2013

leakage and aliasing. This energy integral method consists of recovering equivalent-water thickness of juxtaposed 2° or 4° geographical tiles by inversion of Differences of Potential Anomaly (DPA) between GRACE vehicles A and B that are related to the GRACE inter-satellite KBR Range (KBRR) residuals (Ramillien et al., 2011, 2012). These KBRR residuals were obtained by correcting the raw observations from the a priori gravitational accelerations of known large-scale mass variations (i.e. atmosphere and oceanic mass variations, polar movements, as well as solid and oceanic tides) during the iterative least-squares orbit adjustment made by GINS software (Bruinsma et al., 2010). The effects of non-conservative forces measured by on-board GRACE accelerometers are also removed from the along-track observations, in order to extract the contributions of not modelled phenomena, thus mainly water mass changes in continental hydrology. Since classical gravimetric inversion does not provide a unique solution and to reduce the spurious effects of the noise in the observations, regularization strategies have been proposed to find numerically stable solutions, either based on Singular Value Decomposition (SVD) and *L* curve analysis (Ramillien et al., 2011), or by introducing averaging radius as spatial constraints (Ramillien et al., 2012). Time series of successive 10 day regional solutions of water mass have been produced over a region included the whole Australia [112° E 156° E; 44° S 10° S]. In addition, for solving the problem of the important long wavelength differences between DPA segments and stabilizing the inversion, low-degree polynomials are simply removed from each north–south DPA track to reduce long-term orbit error. Obviously, the risk of this operation is to loose useful long wavelength water mass signals that extensions exceed the dimensions of the considered region. The numerical estimations show us that the predicted regional solutions need to be completed by long wavelength components for comparison with other data sets, when the geographical region is not large enough to contain these long gravity undulations (for more details see Ramillien et al., 2012).

Preliminary tests were made to determine the harmonic degree of Level 2 GRGS solutions to be used to complement short and medium wavelength regional solutions (Fig. 2). The degree of 6 explains mostly the RMS difference between global and

HESSD
10, 5355–5395, 2013

regional solutions. This optimal degree corresponds roughly to the latitudinal extension of the region (≈ 6700 km). Before being added to the inverted GRACE signals, the long wavelength GRGS components represent about 47 and 45 % of the complete hydrological signals over Australia and the Murray–Darling Basin in particular, respectively. As presented in Fig. 3 from December 2008 to November 2009, these seasonal amplitudes of the augmented 10 day regional solutions are typically of ±250 mm of EWH in the tropical Northern region of Australia where the regular monsoon occurs in January and April, yielding an alternation of wet and dry seasons. As expected, these strongest seasonal amplitudes are in the northern tropical band, for latitudes greater than −20° S. Moreover, the series of the regional TWS maps also reveals the constant loss of groundwater in the southeastern part of Australia which is affected by a drought until 2010. During the dry period in the central desert (e.g. January to June 2006, where the cumulated rainfall over six consecutive months remains less than 60 mm), the amplitudes of our regional solutions remain lower than 30 mm of EWH (Fig. 4). As the expected values in this desert area should be small for this 6 month period, these recovered TWS amplitudes can be also considered as an indicator of the level of uncertainty on our prediction.

2.1.2 Global Level 2 solutions from GRGS

To assess the differences of using regional approach instead of global solutions or techniques we compare the solutions derived from integral energy approach to GRGS global solutions. The Level 2 GRGS-EIGEN-GL04-10-day models are derived from Level 1 GRACE measurements including KBRR and from LAGEOS-1/2 SLR data for enhancement of lower harmonic degrees (Bruinsma et al., 2010). These gravity fields are expressed in terms of normalized spherical harmonic coefficients from degree 2 up to degree 50 using an empirical stabilization approach without any smoothing or filtering.

In our study spatial means of Total Water Storage over an specific drainage basin as Murray–Darling will be used in Sect. 3. We remember that for estimating the spatial

HESSD
10, 5355–5395, 2013

means from the spherical harmonics approach, it is suitable to use the formula proposed earlier by Wahr et al. (1998) and Ramillien et al. (2006b). We computed the corresponding variation of water volume inside the basin, $\delta\psi(\Delta t)$, as the scalar product of the water mass coefficients δC_{nm}, δS_{nm} with A_{nm} and B_{nm} the normalized harmonic coefficients of the considered geographical mask:

$$\delta\psi(\Delta t) = 4\pi R^2 \sum_{n=1}^{N} \sum_{m=0}^{M} (A_{nm}\delta C_{nm}(\Delta t) + B_{nm}\delta S_{nm}(\Delta t)) \quad (1)$$

where R is the Earth's mean radius (6371 km). TWS variations can be expressed in terms of equivalent water height changes if $\delta\psi$ is divided by the area of the drainage basin.

10 day Total Water Storage (TWS) grids of 1° spatial resolution are available for 2002–2011 at http://grgs.obs-mip.fr.

2.1.3 Global Level 2 solutions from CSR, GFZ and JPL filtered using ICA approach

A post-processing method based on Independent Component Analysis (ICA) was applied to the Level 2 GRACE solutions from different official providers (i.e. UTCSR, JPL and GFZ) pre-filtered with 400 km radius Gaussian filters. This approach does not require a priori information, except the assumption of statistical independence between the elementary sources that compose the measured signals (i.e. useful geophysical signals plus noise). Separation consists of solving a linear system relating the GRACE solutions provided for a given month, to the unknown independent sources. The contributors to the observed gravity field are forced to be uncorrelated numerically by imposing diagonal cross-correlation matrices. Time series of ICA-based global maps of continental water mass changes from combined UTCSR, JPL and GFZ GRACE solutions, computed over the period March 2003–December 2010, are used in this study. For a given month, the ICA-filtered solutions only differ from a scaling factor, so that

HESSD
10, 5355–5395, 2013

the GFZ-derived ICA-filtered solutions are only presented. The efficiency of the ICA in separating gravity signals from noise by combining Level 2 GRACE solutions has previously been demonstrated over land (Frappart et al., 2010, 2011).

2.2 In-situ data and modelled hydrological datasets

2.2.1 BoM rainfall product

To validate our regional solutions, we compared them to the rainfall over Australia. We use the monthly grids provide by the Bureau of Meteorology of the Australian Government (BoM). which provides rainfall grids expressed as Equivalent Water Height values for the whole of Australia since 1967 (http://www.bom.gov.au). The rainfall product is based on observations of irregularly distributed weather stations. They are averaged to monthly values and interpolated to geographic grids with the spatial resolution of 15′ by 15′ covering the region 111°45′ E to 156°30′ E in longitude and 9°45′ S to 44°45′ S in latitude. The interpolation of the irregular data is based on the Barnes successive-correction method (Jeffrey et al., 2001).

2.2.2 Murray–Darling datasets

Groundwater

In situ estimates of groundwater storage (GWS) in the Murray–Darling Basin were obtained from an analysis of groundwater levels observed in government monitoring bores from 2002 to 2009. Assuming that (1) the shallow aquifers across the Murray–Darling drainage basin are hydraulically connected and that (2) at a large scale the fractured aquifers can be assimilated to a porous media, changes in groundwater storage across the area can be estimated from observations of groundwater levels (e.g. Strassberg et al., 2007). Variations in groundwater storage (ΔS_{GW}) were estimated from in situ measurements as:

HESSD
10, 5355–5395, 2013

$$\Delta S_{GW} = S_y \Delta H \quad (2)$$

where S_y is the aquifer specific yield (%) and H is the groundwater level (L^{-1}) observed in monitoring bores. Groundwater level data (H) were sourced from Government departments of the States covered by the Murray Darling Basin (QLD, Natural Resources and Mines; NSW, Department of Water and Energy; VIC, Department of Sustainability and Environment; and SA, Department of Water Land and Biodiversity Conservation). Only observation bores (production bores excluded) with an average saturated zone < 30 m from the bottom of the screened interval were selected as deeper bores can reflect processes occurring on longer time scales (Fetter, 2001). In the Murray and Darling drainage basins changes in groundwater levels were computed at three and six months time step respectively. Only bores with at least 80 % of the time periods populated with groundwater levels were selected for the analysis (1470 bores in the Murray and 958 bores in the Darling, Fig. 1). The median of the groundwater level for each time period was first calculated at each bore and change at a bore was computed as the difference of median groundwater level between two consecutive periods. A spatial interpolation of the groundwater level change between two consecutive periods was performed across the basin using a kriging technique. Spatial averages of groundwater level change were computed for each aquifer group. The Murray–Darling drainage basin comprises several unconfined aquifers that can be regrouped into 3 groups according to their lithology. The specific yield S_y in Eq. (2) is estimated for each group: to range from 5 to 10%: for the clayey sand unconfined aquifer group (Macumber, 1999; Cresswell et al., 2003; Hekmeijer and Dawes, 2003a; CSIRO, 2008); from 10 to 15 %; for the shallow sandy clay unconfined aquifer group (Macumber, 1999; Urbano et al., 2004); and from 1 to 10 % for the fractured rock aquifer group (Cresswell et al., 2003; Hekmeijer and Dawes, 2003b; Smitt et al., 2003; Petheram et al., 2003). In-situ estimates of changes in GW storage are calculated using the spatially averaged change in groundwater level for aquifer group and the mean value of the specific yield for that

HESSD
10, 5355–5395, 2013

group. The range of possible values for the specific yield was used to estimate the uncertainty. Groundwater changes in the deep, confined aquifers (mostly Great Artesian Basin and Renmark aquifers) are either due to: (1) a change in groundwater recharge at unconfined outcrop; (2) shallow pumping at unconfined outcrop or (3) deep pumping in confined areas for farming (irrigation and cattle industry). Total pumping from the deep, confined aquifers was estimated to amount to $-0.42\,km^3\,yr^{-1}$ in 2000 (Ife and Skelt, 2004) while groundwater pumping across the basin was $-1.6\,km^3$ in 2002–2003 (Kirby et al., 2006). To allow direct comparison between TWS and in-situ GW estimates, pumping from the deep aquifers was added to the in-situ GW time series assuming the $-0.42\,km^3\,yr^{-1}$ pumping rate remained constant during the study period.

Surface water

In the predominantly semiarid Murray–Darling Basin, most of the surface water (SW) stored in a network of reservoirs, lakes and weirs (Kirby et al., 2006). A daily time series of the surface water storage in the network of reservoirs, lakes, weirs and in-channel storage was obtained from the Murray–Darling Basin Commission and the state governments from 2002 to 2011.

Soil moisture from AWRA model

Soil moisture was derived from the Australian Water Resources Assessment (AWRA) hydrologic model (Van Dijk and Renzullo, 2010; Van Dijk et al., 2011). The system combines a comprehensive spatial hydrological model with meteorological forcing data and remotely sensed land surface properties.

2.2.3 Fitzroy streamflow dataset

A times series of monthly streamflow values spanning from 1998 to 2011 was obtained at two gauging stations along the Fitzroy River. The observations at Willare and

HESSD
10, 5355–5395, 2013

Noonbakhan stations (see Fig. 1) were provided by the departement of water (DoW) of the Governement of Western of Australia (www.water.wa.gov.au).

3 Results and discussion

3.1 PCA of the GRACE data sets

PCA was applied to the TWS time series of the 10 day GRACE-based regional, 10 day GRGS RL02 and monthly ICA 400 km filtered solutions, as well as the BoM rainfall grids after having removed the dominant seasonal cycle using an averaging window of 13 months. Figures 5, 7 and 9 present the spatial components of the three first modes that correspond to the most significant variability. The temporal components are presented in Figs. 6, 8 and 10. The three first mode of PCA explained a variance of 60, 13 and 15 % of variability respectively. Correlation values between the first modes of the different datasets are shown in Table 1 for the spatial patterns and Table 2 for the temporal patterns and they will be discussed in the next sections.

3.1.1 The first mode of TWS variability

The first PCA mode explains 60, 67 and 52 % for the regional, GRGS and ICA 400 km filtered TWS solutions, respectively. The first spatial component of GRGS solutions still contains important north–south striping (Fig. 5) that degrades amplitudes and localizations of the structures. Note that the regional approach reduces this polluting noise due to orbit resonance by construction, since its first step consists of removing the long-term satellite gravity undulations before inversion for equivalent-water heights, as explained in Sect. 2.1.1. For each PCA mode, the correlations between the spatial components of GRACE base datasets and rainfall BoM product are shown in Table 1. Cross-correlations values for temporal components are also estimated and presented in Table 2. For the first mode, temporal patterns correlations between different GRACE solutions are in a good agreement (70–80 %). However, comparing GRACE data with

HESSD
10, 5355–5395, 2013

rainfall product, only around 60 % of the signal are explained. In fact, GRACE satellites observe the mass variations due to rainfall but also other mass redistributions through the water balance equation. On the other hand, the correlation between the spatial patterns of GRACE products and rainfall drop due to the loss of mass only observed in the gravity field solutions at the Great Sandy Desert (at the northwest region of Australia) and the Murray Basin. In the Great Sandy desert, rainfall is nearly ungauged (Van Dijk et al., 2011) and discrepancies are due to the missing information in the BoM products. The signal observed over Murray basin could be associated to aquifer variations. The loss of mass over Murray–Darling Basin presented in the spatial component of the first mode (Fig. 5) are due to the recent Millennium drought affecting this region (Leblanc et al., 2009, 2011). The corresponding negative trend on the temporal component can be related to the increase of the drought from 2003 to 2009. The trend of water mass changes after 2010 indicates a gain of water mass in the southeastern part.

The South Oscillation Index (SOI) and the Pacific Decadal Oscillation (PDO) interannual variations were smoothed out using the same 13 month averaging window, and then compared to the temporal components of the first modes (Fig. 6a and b). As illustrated by Table 3, high correlations (≈ 70 %) were found between these climatic indexes and the temporal components of the first TWS modes, suggesting the important influence of these climate oscillations on the Australian water mass storage at interannual time scales. Mantua and Hare (2002) compared PDO with rainfall data and suggested that warm phases of the PDO (positive values) coincide with anomalously dry periods in eastern Australia. The signature of this phenomena can be seen in the spatial and temporal components of the first mode of the PCA int the Murray–Darling basin (Figs. 5 and 6) and it is probably the reason of the large negative correlations values obtained in Table 3.

The signifcant correlations obtained for the SOI and PDO suggest that the Australian climat confirm that Australia climate is forced by these climate oscillations at interannual scales. In addition, water mass content reduction over central and southern regions of

HESSD
10, 5355–5395, 2013

Australia seems to be also associated to IOD positive phases as previously suggested by García-García et al. (2010).

3.1.2 The second and third modes

In the case of our regional solutions, the second and third modes have very close explained variances (i.e. 13 and 15 %, respectively), so we decided to inverse their order for consistency with the modes from other solutions.

The PCA spatial patterns of second mode of GRGS, ICA, rainfall data and third mode of regional solutions presented in Fig. 7 show an important and continuous deficit of mass occuring over the Murray–Darling and Lake Eyre regions. Looking at the temporal components in Fig. 8a, we notice that the strongest deficit happened in April 2006 and it can be interpreted as the maxima of severity of the Millennium drought that has been observed in year 2006 (Leblanc et al., 2011).

However, the low correlation values (spatial or temporal, see Tables 1 and 2) between GRACE products and rainfall over the whole Australia seem to indicate that the main amplitudes seen in the southeast part of Australia are due to other hydrological processes. In fact, a significant amplitude is located at Murray–Darling basin (Fig. 7 spatial pattern and Fig. 8a temporal pattern) and probably linked to the interannual groundwater level variations. For this purpose we derived groundwater internannual signal from in situ observations for comparison (see Sect. 1.2). They are obtained by computing the average of observations over the Murray–Darling Basin, after the seasonal variations are removed using an averaging window. The water mass rate over the observation period 2003–2010 are essentially presented in the first mode components, as in the previous section. Then, the linear trend is also removed from groundwater observations in order to compare to the second mode temporal component. Signals are shown in Fig. 8a and b. Cross-correlation values are significant for the regional estimates (61 %) and GRGS solutions (73 %) with 4 months of time lag. In the case of ICA solutions, the correlation is lower and about 40 % with a 5 months of time lag. The spatial PCA modes presented in Figs. 9 and 10a for temporal modes show positive

HESSD
10, 5355–5395, 2013

variations located in the North-West part of Australia which correspond to a gain of water mass related to an increase of rainfall (Li et al., 2009). As previously mentioned by Munier et al. (2012), an inter-annual cycle of TWS appears over the Fitzroy basin region. This long-term undulation in the GRACE modes shown in Figs. 9 and 10a is consistent with the third mode of rainfall (see correlation values in Tables 1 and 2). Cross-correlations values are 64, 50 and 74 % for regional, GRGS and ICA solutions respectively and with a time lag of 4 months with respect to rainfall data. Moreover, discharge records of Willare and Noonkanbah stations along the Fitzroy river have quasi-periodic peaks of water level in 2004, 2006 and 2008 (Fig. 10b), excepting for 2010. These maxima of river discharge coincide quite well with the ones seen on the GRACE temporal mode, although the signature of the high Fitzroy river discharge of 2009 is hardly present in GRACE data.

3.2 Localization of hydrological event

To demonstrate the improvement in detection brought by our regional solutions, we confronted them with known meteorological events sharply localized in both space and time.

3.2.1 Exceptional rainfall in 2010

Anomaly maps of TWS were generated as the difference between the monthly TWS grids corresponding to the exceptionally high rainfall in the central desert (from July to September 2010), and the grid averaged over the previous dry season (i.e. mean of the six months from June to November 2009). GRACE-based TWS and BoM rainfall anomaly grids are presented in Fig. 11. When the BoM rainfall anomaly grids are taken as a reference, TWS anomaly grids from regional solutions offer a better spatial localization of the September 2010 rainfall structures than the anomalies computed with global GRGS solutions.

HESSD
10, 5355–5395, 2013

3.2.2 Detection of the cyclone Charlotte

The heavy rainfall and subsequent floods that were caused by the cyclone Charlotte between the 9 and 12 January 2009, in the Gulf of Carpentaria Basins, are clearly visible in Fig. 12. Tregoning et al. (2012) have already noticed the signature of this climate event in GRACE global solutions. The first flood warnings for Queensland were issued in the first week of January from moderate to major flooding in the Gulf rivers, and Georgina and Diamantina rivers in Western Queensland (see Fig. 1). Since important rainfall continued, these warnings were maintained for nine weeks (see BoM report of 2009). Instantaneous TWS anomalies, defined as the difference of two consecutive TWS 10 day regional and GRGS RL02 solutions are presented in Fig. 12a and b respectively. In Fig. 12c TWS anomalies for ICA solutions defined as the difference of two consecutive TWS monthly solutions. We notice clearly the strong signature of the floods caused by the cyclone Charlotte, since the regional solutions reveal important positive water heights of ≈ 600 mm of EWH, higher than the levels observed in the previous months. For our regional solutions, this corresponding TWS anomaly is localized precisely in the Carpentaria drainage basins area (see Fig. 1). This sudden meteorological event agrees well with the BoM rainfall data (Fig. 12d) and GRGS RL02 estimates. However, ICA solutions show a very low amplitude of this event.

3.3 Basin-averaged time series of TWS

Leblanc et al. (2011) have shown the effects of drought over Murray–Darling Basin and they compared GRGS-RL02 global solutions to thus obtained as the sum of in situ data for surface and ground waters and model outputs for soil moisture over the basin for a the period 2002–2010.

In our analysis in order to validate the regional approach, we compared the regional and GRGS RL02 solutions and we included the ICA solutions. A comparison of time series of GRACE TWS averaged over the whole Murray–Darling using GRGS RL02, ICA and the regional solutions is presented in Fig. 13. We notice TWS variations

HESSD
10, 5355–5395, 2013

are consistent between all GRACE solutions (correlations values: ICA/regional = 65 %, ICA/GRGS = 70 %, regional/GRGS = 90 %).

The average of rainfall in 2010, causde by a switch to a strong La Niña event, brings the end to this prolonged drought and leading the increase in TWS.

For comparison GRACE-based products with other independent datasets, we used the soil moisture outputs from AWRA Australian hydrological model and bores localizations are extended then we have a better spatial coverage of groundwater level variations than in the case of the previous study of Leblanc et al. (2011). To make their spatial resolution compatible to the one of the regional GRACE solutions, TWS estimates reconstructed from in-situ and modelled hydrologic information were interpolated onto 2° sampling grids. According to the temporal resolution of the GW data for the period of 2003–mid 2009, the GRACE datasets were smoothed versus time: 3 month and 6 month samplings for Murray and Darling basins, respectively. The corresponding time series for the Murray and Darling Basins are presented in Fig. 14. Correlations of 0.7–0.9 and RMS values of 15–30 mm EWH from Table 4 suggest a good agreement between re-constructed TWS (i.e. SM + SW + GW) variations and the ones from GRACE data sets, our regional GRACE solutions giving better results. As seen in Fig. 14, we used a coefficient of proportionality (i.e. specific yield) ranging from 0.06 to 0.15 to convert in situ measurements of water table into water content variations, which are slightly larger but very comparable to the GRACE-based amplitudes. Gridded correlations and RMS differences in the Murray–Darling Basin are even better for the regional GRACE solutions (Fig. 15), especially in the Murray Basin where the correlations are greater than 75 % and GW measurements are the densest (see Fig. 1); GRGS and ICA solutions may drop down to 25 % and even less.

HESSD
10, 5355–5395, 2013

4 Conclusions

In this paper, we validated our 10 day GRACE regional solutions of water mass variations over Australia for the period 2003–2011 by comparing them with (i) global GRGS RL02 and ICA 400 km solutions based on spherical harmonics representation, and (ii) independent datasets, i.e. estimates of rainfall, groundwater and surface water derived from in-situ observations and modelled soil moisture. Once applied to the GRACE data sets, PCA provided the main modes of variability of these solutions. Temporal and spatial patterns are consistent for the regional and global solutions. However, the regional solutions offer better geographical localization of hydrological structures, while global solutions remain polluted by aliasing errors (i.e. North–South striping). High correlations between SOI and PDO climate indexes during the Millennium Drought and our regional solutions exist, in particular for the first PCA mode. Second and third modes are also related to the drought that occurred in the southeastern part of Australia up to 2006. While all the GRACE solutions remain consistent over Australia, our regional solutions yield the best agreement with in situ water table measurements in the Murray–Darling drainage Basin.

Acknowledgements. Lucia Seoane's work was funded by ARC discovery projet at James Cook University (Australia). We would like to thank Adam Fakes for providing groundwater grids derived from in-situ measurements.

The publication of this article is financed by CNRS-INSU.

References

Andersen, O. B., Seneviratne, S. I., Hinderer, J., and Viterbo, P.: GRACE-derived terrestrial water storage depletion associated with the 2003 European heat wave, Geophys. Res. Lett., 32, L18405, doi:10.1029/2005GL023574, 2005.

Awange, J., Sharifi, M., Baur, O., Keller, W., Featherstone, W., and Kuhn, M.: GRACE hydrological monitoring of Australia: Current limitations and future prospects, J. Spatial Sci., 54, 23–36, doi:10.1080/14498596.2009.9635164, 2009.

Awange, J., Fleming, K. M., Kuhn, M., Featherstone, W. E., Heck, B., and Anjasmara, I.: On the suitability of the 4 × 4 GRACE mascon solutions for remote sensing Australian hydrology, Remote Sens. Environ., 115, 864–875, doi:10.1016/j.rse.2010.11.014, 2011.

BoM report: Queensland Floods January and February 2009, Bureau of Meteorology, Queensland, Australia, 2009.

Bruinsma, S., Lemoine, J.-M., Biancale, R., and Valès, N.: CNES/GRGS 10-day gravity models (release 2) and their evaluation, Adv. Space Res., 45, 587–601, doi:10.1016/j.asr.2009.10.012, 2010.

Cresswell, R. G., Dawes, W. R., Summerell, G. K., and Walker, G. R.: Assessment of salinity management options for Kyeamba Creek, New South Wales: Data analysis and groundwater modelling, CSIRO Land and Water Technical Report 26/03, Murray Darling Basin Commission, Canberra, 2003.

CSIRO Report: Water availability in the Loddon-Avoca, A report to the Australian Government from the CSIRO Murray-Darling Basin Sustainable Yields Project, Published by CSIRO, Australia, 123 pp., 2008.

Fetter, C. W.: Applied Hydrogeology, Published by Prentice Hall Inc, Upper Saddle River, New Jersey, 07458 USA, 2001.

Forootan, E. and Kusche, J.: Separation of global time-variable gravity signals into maximally independent components, J. Geodesy, 86, 477–497, doi:10.1007/s00190-011-0532-5, 2012.

Frappart, F., Ramillien, G., Maisongrande, P., and Bonnet, M.-P.: Denoising satellite gravity signals by independent component analysis, IEEE Geosci. Remote Sens. Lett., 7, 421–425, doi:10.1109/LGRS.2009.2037837, 2010.

Frappart, F., Ramillien, G., Leblanc, M., Tweed, S. O., Bonnet, M.-P., and Maisongrande, P.: An independent Component Analysis approach for filtering continental hydrology in the GRACE gravity data, Remote Sens. Environ., 115, 187–204, 2011.

HESSD
10, 5355–5395, 2013

Frappart, F., Papa, F., Santos da Silva, J., Ramillien, G., Prigent, C., Seyler, F., and Calmant, S.: Surface freshwater storage and dynamics in the Amazon basin during the 2005 exceptional drought, Environ. Res. Lett., 7, 044010, doi:10.1088/1748-9326/7/4/044010, 2012.

Frappart, F., Ramillien, G., and Ronchail, J.: Changes in terrestrial water storage versus rainfall and discharges in the Amazon basin, Int. J. Climatol., online first, doi:10.1002/joc.3647, 2013.

García-García, D. C., Ummenhofer, C., Zlotnicki, V.: Australian water mass variations from GRACE data linked to Indo-Pacific climate variability, Remote Sens. Environ., 115, 2175–2183, doi:10.1016/j.rse.2011.04.007, 2011.

Hekmeijer, P. and Dawes, W.: Assessment of salinity management options for South Loddon Plains, Victoria: Data analysis and groundwater modeling, CSIRO Land and Water Technical Report 24/03, Published by Murray-Darling Basin Commission, Canberra, Australia,, 2003a.

Hekmeijer, P. and Dawes, W.: Assessment of salinity management options for Axe Creek, Victoria: Data analysis and groundwater modelling, CSIRO Land and Water Technical Report 22/03, MDBC Publication 08/03, Published by Murray-Darling Basin Commission, Canberra, Australia, 40 pp., 2003b.

Houborg, R., Rodell, M., Li, B., Reichle, R., and Zaitchik, B. F.: Drought indicators based on model-assimilated Gravity Recovery and Climate Experiment (GRACE) terrestrial water storage observations, Water Resour. Res., 48, W07525, doi:10.1029/2011WR011291, 2012.

Ife, D. and Skelt, K.: Murray-Darling Basin Groundwater Status, Murray-Darling Basin Commission, publication 32/04, Canberra, ISBN 1876830948, 2004.

Jeffrey, S. J., Carter, J. O., Moodie, K. B., and Beswick, A. R.: Using spatial interpolation to construct a comprehensive archive of Australian climate data, Environ. Model. Softw., 16, 309–330, 2001.

Klees, R., Revtova, E. A., Gunter, B. C., Ditmar, P., Oudman, E., Winsemius, H. C., and Savenije, H. H. G.: The design of an optimal filter for monthly GRACE gravity models, Geophys. J. Int., 175, 417–432, doi:10.1111/j.1365-246X.2008.03922.x, 2008.

Kirby, M., Evans, R., Walker, G., Cresswell, R., Coram, J., Khan, S., Paydar, Z., Mainuddin, M., McKenzie, N., and Ryan, S.: The shared water resources of the Murray–Darling Basin, Publication 21/06, available online at: http://www.mdbc.gov.au, Murray–Darling Basin Commission, Canberra, 2006.

HESSD
10, 5355–5395, 2013

Leblanc, M., Tregoning, P., Ramillien, G., Tweed, S., and Fake, A.: Basin scale, integrated observations of the early 21st Century multi-year drought in southeast Australia, Water Resour. Res., 45, W04408, doi:10.1029/2008WR007333, 2009.

Leblanc, M., Tweed, S., Ramillien, G., Tregoning, P., Frappart, F., Fakes, A., and Cartwright, I.: Groundwater change in the Murray basin from long-term in-situ monitoring and GRACE estimates, in: Climate change effects on groundwater resources: A global synthesis of findings and recommendations, edited by: Treidel, H. and Gurdak, J. J., CRC Press, 169–187, 2011.

Li, L. T., Donohue, R. J., McVicar, T. R., Van Niel, T. G., Ten, J., Potter, N. J., Smith, I. N., Kirono, D. G. C., Bathols, J. M., Cai, W., Marvanek, S. P., Gallant, S. N., Chiew, F. H. S., and Frost, A. J.: Climate data and their characterisation for hydrological scenario modelling across northern Australia. A report to the Australian Government from the CSIRO Northern Australia Sustainable Yields Project. Published by CSIRO Water for a Healthy Country Flagship, Australia, 63 pp., 2009.

Macumber, P. G.: Groundwater flow and resource potential in the Bridgewater and Salisbury West GMAs, Phillip Macumber Consulting Services, Melbourne, 88 pp., 1999.

Mantua, N. J. and Hare, S. R.: The Pacific Decadal Oscillation, J. Oceanogr., 58, 35–44, 2002.

Munier, S., Becker, M., Maisongrande, P., and Cazenave, A.: Using GRACE to detect Groundwater Storage variations: the cases of Canning Basin and Guarani aquifer system, Int. Water Technol. J., Vol. 2, 2012.

Petheram, C., Dawes, W., Walker, G., and Grayson, R. B.: Testing in class variability of groundwater systems: Local upland systems, Hydrol. Process., 17, 2297–2313, doi:10.1002/hyp.1333, 2003.

Ramillien, G., Frappart, F., Güntner, A., Ngo-Duc, T., Cazenave, A., and Laval, K.: Time variations of the regional evapotranspiration rate from Gravity Recovery and Climate Experiment (GRACE) satellite gravimetry, Water Resour. Res., 42, W10403, doi:10.1029/2005WR004331, 2006a.

Ramillien, G., Lombard, A., Cazenave, A., Ivins, E. R., Llubes, M., Remy, F., and Biancale, R.: Interannual variations of the mass balance of the Antarctica and Greenland ice sheets from GRACE, Global Planet. Change, 53, 198–208, doi:10.1016/j.gloplacha.2006.06.003, 2006b.

Ramillien, G., Biancale, R., Gratton, S., Vasseur, X., and Bourgogne, S.: GRACE-derived surface mass anomalies by energy integral approach, Application to continental hydrology, J. Geodesy., 85, 313–328, doi:10.1007/s00190-010-0438-7, 2011.

HESSD
10, 5355–5395, 2013

Ramillien, G., Seoane, L., Frappart, F., Biancale, R., Gratton, S., Vasseur, X., and Bourgogne, S.: Constrained regional recovery of continental water mass time-variations from GRACE based geopotential anomalies over South America, Surv. Geophys., 33, 887–905 doi:10.1007/s10712-012-9177-z, 2012.

Rieser, D., Kuhn, M., Pail, R., Anjasmara, I. M., and Awange, J.: Relation between GRACE-derived surface mass variations and precipitation over Australia, Aust. J. Earth Sci., 57, 887–900, doi:10.1080/08120099.2010.512645, 2010.

Rodell, M., Famiglietti, J. S., Chen, J., Seneviratne, S. I., Viterbo, P., Holl, S., and Wilson, C. R.: Basin scale estimate of evapotranspiration using GRACE and other observations, Geophys. Res. Lett., 31, L20504, doi:10.1029/2004GL020873, 2004.

Rodell, M., Chen, J., Kato, H., Famiglietti, J. S., Nigro, J., and Wilson, C.: Estimating groundwater storage changes in the Mississippi River basin (USA) using GRACE, Hydrogeol. J., 15, 159–166, doi:10.1007/s10040-006-0103-7, 2007.

Smitt, C., Doherty, J., Dawes, W., and Walker, G.: Assessment of salinity management options for the Brymaroo catchment, South-eastern Queensland, CSIRO Land and Water Technical Report 23/03, Murray-Darling Basin Commission, Canberra, Australia, 2003.

Strassberg, G., Scanlon, B. R., and Rodell, M.: Comparison of seasonal terrestrial water storage variations from GRACE with groundwater-level measurements fromthe High Plains Aquifer (USA), Geophys. Res. Lett., 34, L14402, doi:10.1029/2007GL030139, 2007.

Swenson, S. C. and Wahr, J.: Post-processing removal of correlated errors in GRACE data, Geophys. Res. Lett., 33, L08402, doi:10.1029/2005GL025285, 2006.

Syed, T. H., Famiglietti, J. S., Rodell, M., Chen, J., and Wilson, C. R.: Analysis of terrestrial water storage changes from GRACE and GLDAS, Water Resour. Res., 44, W02433, doi:10.1029/2006WR005779, 2008.

Tregoning, P., Lambeck, K., and Ramillien, G.: GRACE estimates of sea surface height anomalies in the Gulf of Carpentaria, Australia, Earth Planet. Sc. Lett., 271, 241–244, doi:10.1016/j.epsl.2008.04.018, 2008.

Tregoning, P., McClusky, S., van Dijk, A. I. J. M., Crosbie, R. S., and Peña-Arancibia, J. L.: Assessment of GRACE Satellites for Groundwater Estimation in Australia, National Water Commission, Canberra, 82 pp., 2012.

Urbano, L. D., Person, M., Kelts, K., and Hanor, J. S. :Transient groundwater impacts on the development of paleoclimatic lake records in semi-arid environments, Geofluids, 4, 187–196, doi:10.1111/j.1468-8123.2004.00081.x, 2004.

HESSD
10, 5355–5395, 2013

van Dijk, A. I. J. M. and Renzullo, L. J.: Water resource monitoring systems and the role of satellite observations, Hydrol. Earth Syst. Sci., 15, 39–55, doi:10.5194/hess-15-39-2011, 2011.
van Dijk, A. I. J. M., Renzullo, L. J., and Rodell, M.: Use of GRACE terrestrial water storage retrievals to evaluate model estimates by the Australian water resources assessment system, Water Resour. Res., 47, W11524, doi:10.1029/2011WR010714, 2011.
Wahr, J., Molenaar, M., and Bryan, F.: Time variability of the Earth's gravity field: hydrological and oceanic effects and their possible detection using GRACE, J. Geophys. Res., 103, 30205–30229, 1998.

HESSD
10, 5355–5395, 2013

Table 1. Correlation values between PCA spatial components (mode 1, 2 and 3) of differents GRACE based datasets and rainfall BoM product.

	Mode 1	Mode 2[a]	Mode 3[b]
Regional solution/GRGS	0.78	0.93	0.88
Regional solution/ICA	0.86	0.87	0.86
GRGS/ICA	0.82	0.83	0.77
Regional solution/rainfall	0.44	0.38	0.50
GRGS/rainfall	0.38	0.24	0.55
ICA/rainfall	0.67	0.62	0.55

[a] Except for regional solutions: here mode 3 is used to estimate correlation values. [b] Except for regional solutions: here mode 2 is used to estimate correlation values.

HESSD
10, 5355–5395, 2013

Table 2. Cross-correlation maxima values and corresponding temporal lag in number of months (second value in italic) between PCA temporal components (mode 1, 2 and 3) of differents GRACE based datasets regional solutions, GRGS and ICA as well as rainfall BoM product. Data derived from Regional and GRGS are filtered and interpolated to monthly resolution. The time lag represents the time delay between water mass variations derived from GRACE and the observed rainfall.

	Mode 1	Mode 2[a]	Mode 3[b]
Regional solution/GRGS	0.98, *0*	0.96, *0*	0.94, *0*
Regional solution/ICA	0.95, *0*	0.93, *0*	0.79, *0*
GRGS/ICA	0.97, *0*	0.89, *0*	0.64, *0*
Regional solution/rainfall	0.59, *–1*	0.19, *6*	0.64, *4*
GRGS/rainfall	0.64, *–1*	0.24, *5*	0.50, *4*
ICA/rainfall	0.70 , *0*	0.33, *1*	0.73, *4*

[a] Except for regional solutions: here mode 3 is used to estimate correlation values. [b] Except for regional solutions: here mode 2 is used to estimate correlation values.

HESSD
10, 5355–5395, 2013

Table 3. Correlation values between climate index and PCA temporal patterns for modes 1, 2 and 3 of regional, GRGS and ICA solutions.

	SOI Index	PDO index
	Mode 1	
Regional	0.73	−0.80
GRGS	0.70	−0.78
ICA	0.74	−0.72

HESSD
10, 5355–5395, 2013

Table 4. Correlation (first value) and RMS of the difference (second value in italic) between time series over Murray and Darling computed from different GRACE solutions and the modeled/in-situ estimates (SM + SW + GW) using the maximum, mean and minimum values of the specific yield. RMS units are mm of EWH.

	Murray		
	Regional	GRGS	ICA
$S_{y_{min}}$	0.92, *16.27*	0.87, *20.27*	0.87, *24.96*
$S_{y_{mean}}$	0.92, *24.03*	0.88, *25.10*	0.85, *36.03*
$S_{y_{max}}$	0.92, *34.35*	0.89, *33.72*	0.84, *47.47*
	Darling		
	Regional	GRGS	ICA
$S_{y_{min}}$	0.71, *12.18*	0.68, *13.40*	0.53, *14.34*
$S_{y_{mean}}$	0.70, *13.17*	0.67, *14.20*	0.48, *16.30*
$S_{y_{max}}$	0.68, *14.63*	0.65, *15.53*	0.43, *18.44*

HESSD
10, 5355–5395, 2013

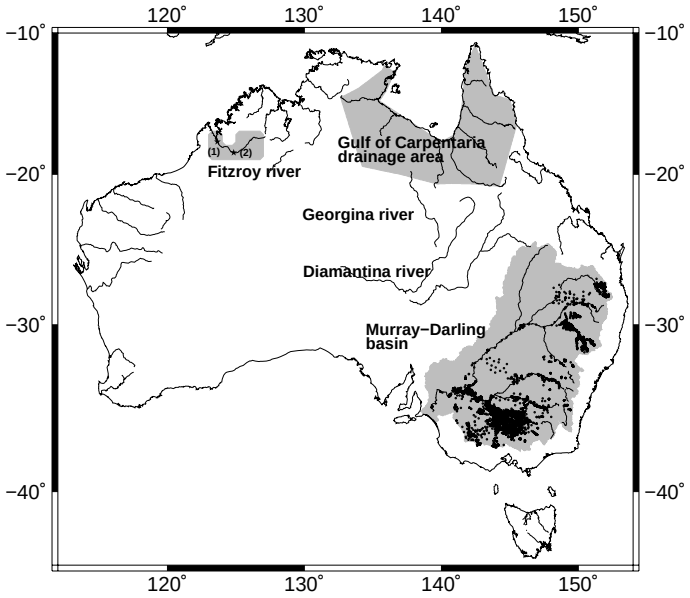

Fig. 1. Australian drainage regions used in our study. At Fitzroy river, two stations (discharge) are considered: (1) Willare station (2) Noonkanbah station. Geographical locations of the bores in the Murray–Darling are marked as black cercles. They represented, with at least 60 % of data period populated (because of their availability during the period 2002–2009), averages of the first 30 m of the water column height.

HESSD
10, 5355–5395, 2013

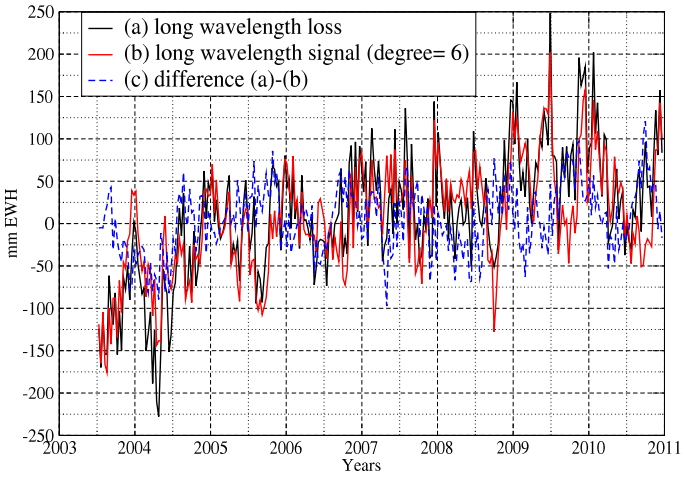

Fig. 2. Water mass time series averaged over Australia: **(a)** difference between regional and GRGS solutions, **(b)** GRGS GRACE solutions up to degree 6, and **(c)** their difference (RMS value 39 mm).

HESSD
10, 5355–5395, 2013

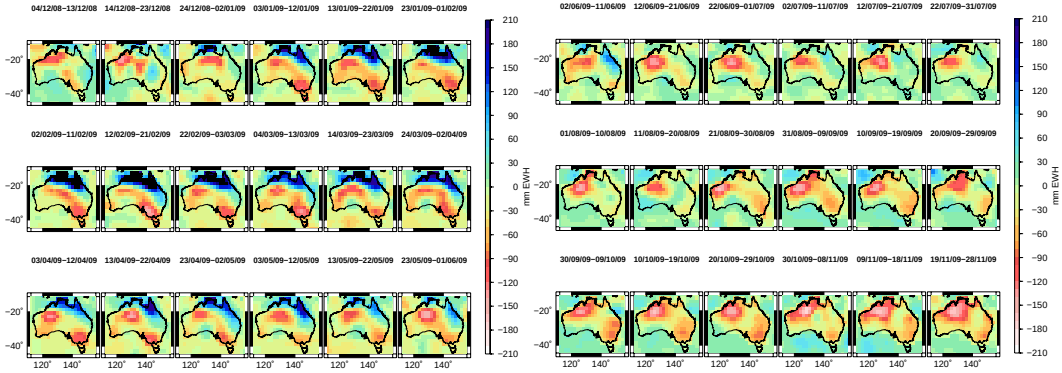

Fig. 3. Time series of regional maps of water mass from December 2008 to November 2009. We can notice the annual signal with amplitude of ±250 mm of EWH representing the alternating wet and dry seasons.

HESSD
10, 5355–5395, 2013

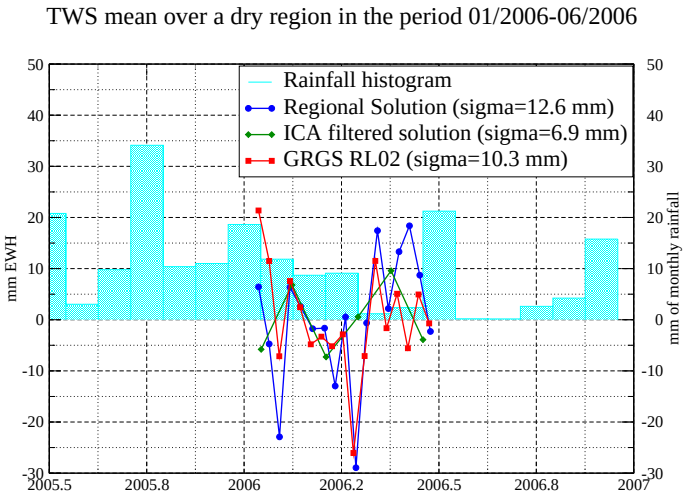

Fig. 4. Time series of TWS means over the estimated desert region (Central Australia) of 18 tiles, the largest signal amplitudes are lesser than 30 mm and the RMS value is of 12.24 mm.

HESSD
10, 5355–5395, 2013

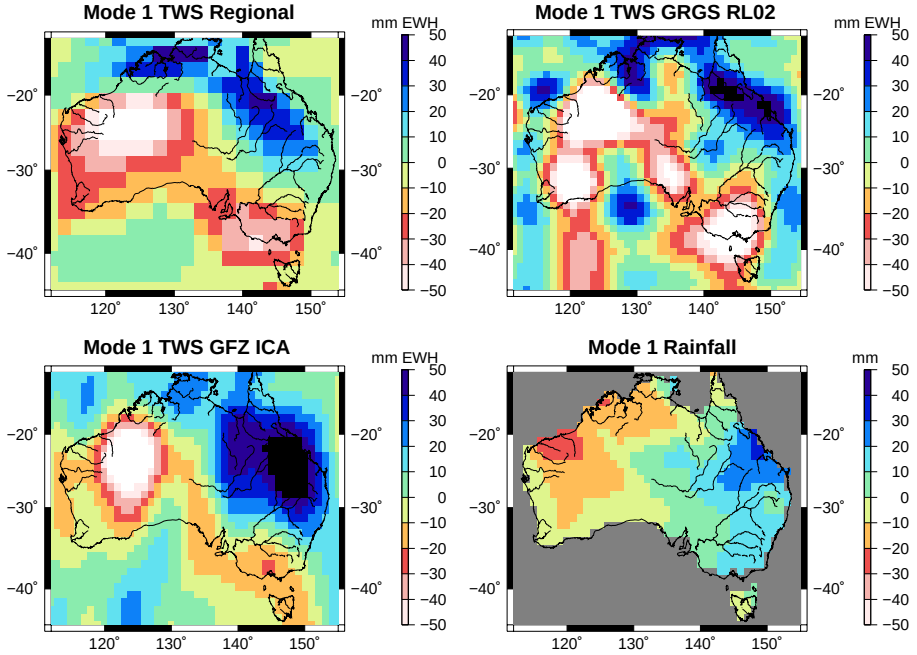

Fig. 5. Spatial components of PCA 1st orthogonal mode.

HESSD
10, 5355–5395, 2013

Regional GRACE-derived water mass variations over Australia

L. Seoane et al.

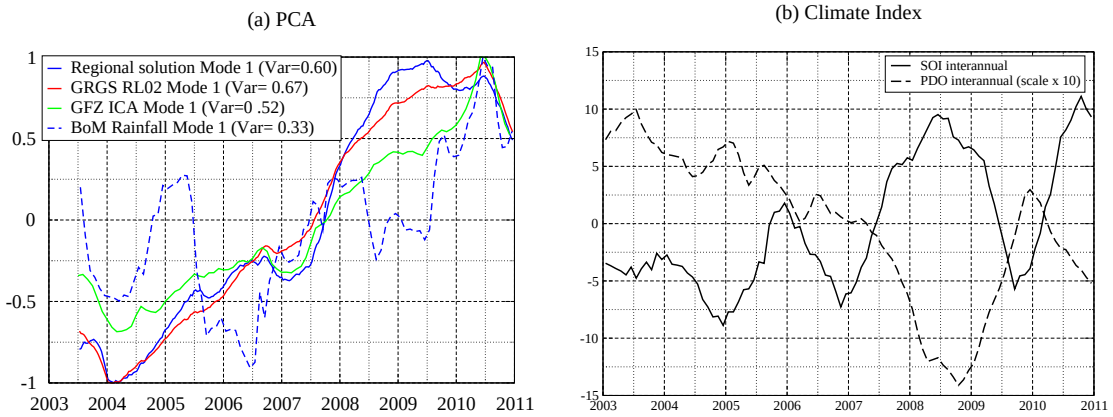

Fig. 6. (a) Temporal components of PCA 1st orthogonal mode. **(b)** Interannual variations of the Southern Oscillation Index (SOI) and Pacific Decadal Oscillation (PDO).

HESSD
10, 5355–5395, 2013

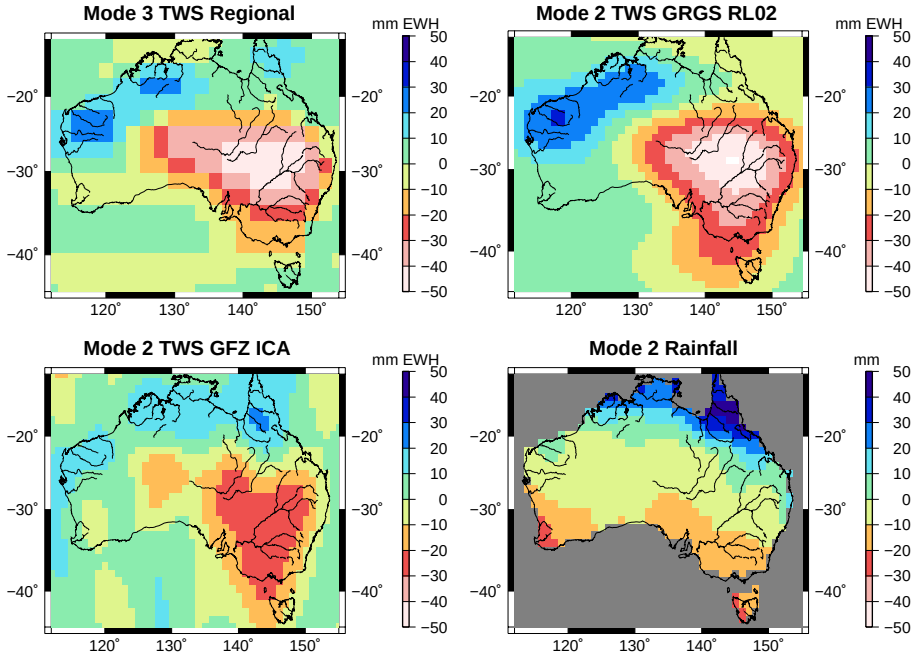

Fig. 7. Spatial components of PCA 3rd orthogonal mode of regional solutions and 2nd mode of GRGS, ICA and Rainfall product.

HESSD
10, 5355–5395, 2013

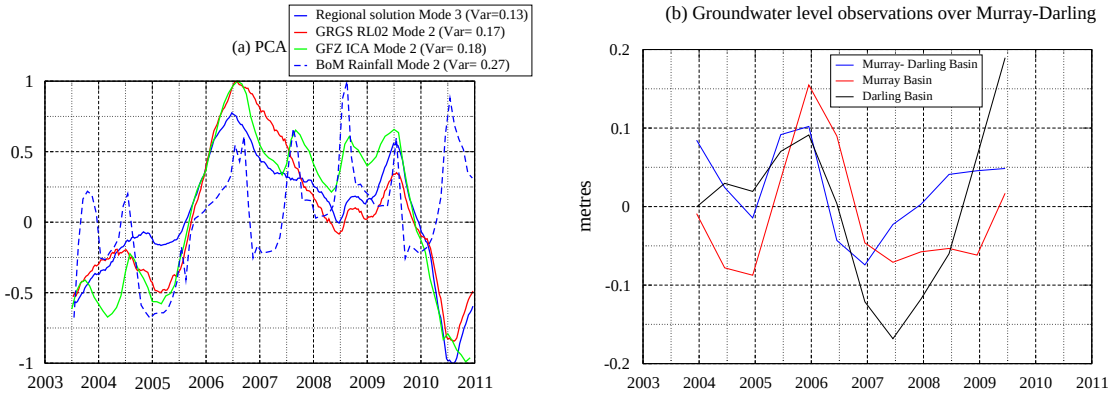

Fig. 8. (a) Temporal components of PCA 3rd orthogonal mode of regional solutions and 2nd mode of GRGS, ICA and Rainfall product. **(b)** Groundwater levels from in-situ measurements over Darling basin.

HESSD
10, 5355–5395, 2013

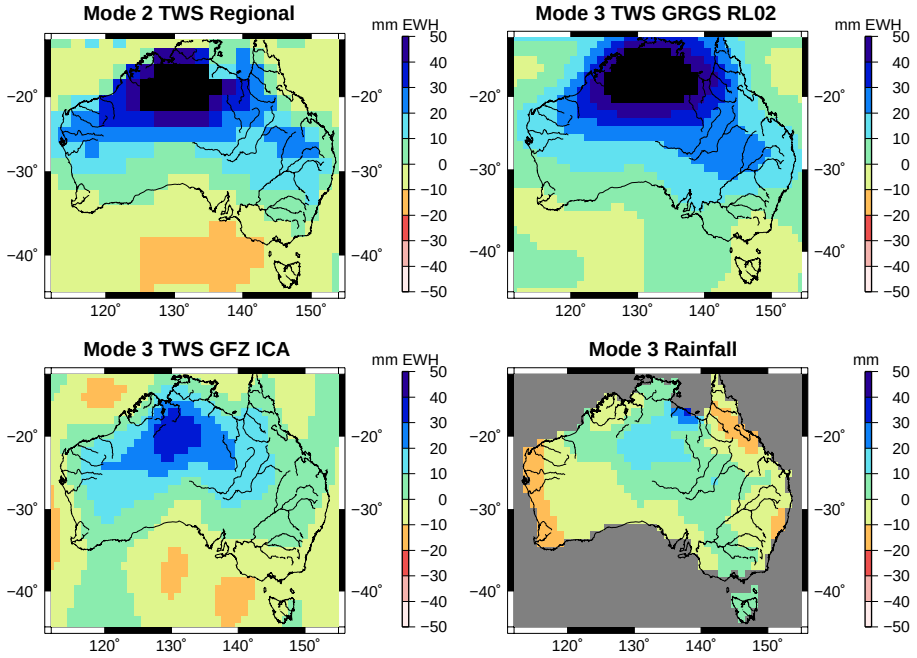

Fig. 9. Spatial components of PCA 2nd orthogonal mode of regional solutions and 3rd mode of GRGS, ICA and Rainfall product.

HESSD
10, 5355–5395, 2013

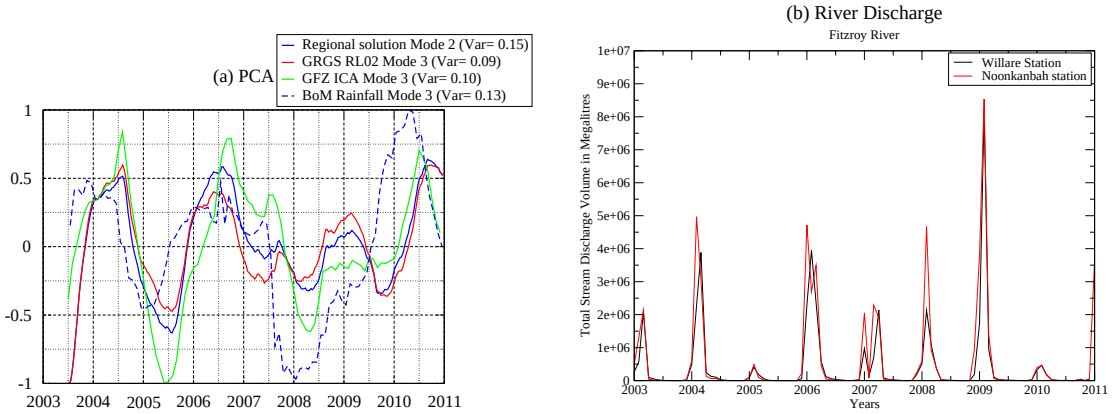

Fig. 10. (a) Temporal components of PCA 2nd orthogonal mode of regional solutions and 3rd mode of GRGS, ICA and Rainfall product. **(b)** In-situ observations of Fitzroy river discharge in MegaLitres (stations Willare and Noonkanbah).

HESSD
10, 5355–5395, 2013

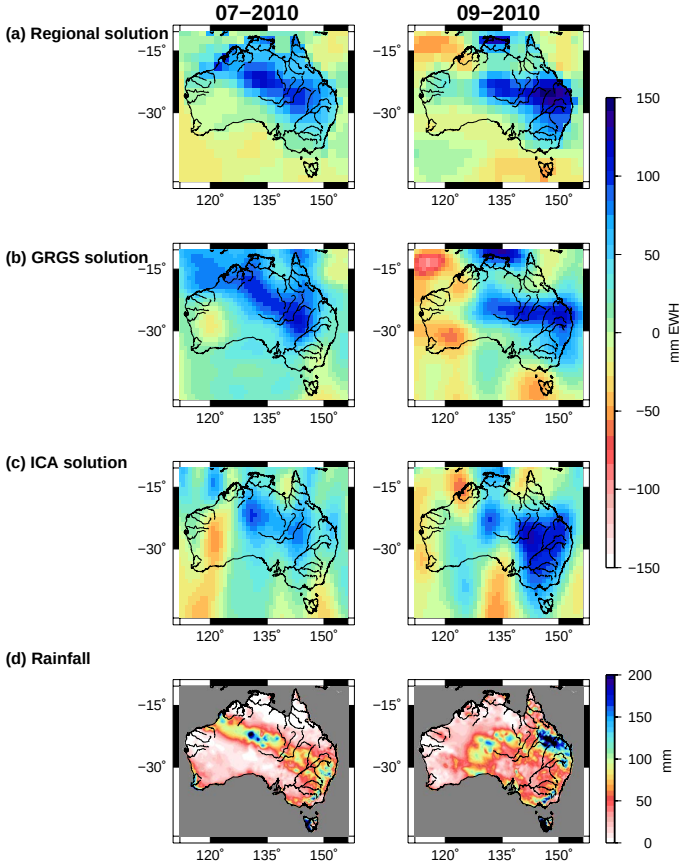

Fig. 11. Regional and GRGS RL02 of ΔTWS monthly maps estimated with respect to the mean map for the previous driest season (from June to November 2009), and rainfall maps. For these two periods we can notice that the regional solutions show a better localization of better the exceptional rainfall maximum ocurring in the central region of Australia.

HESSD
10, 5355–5395, 2013

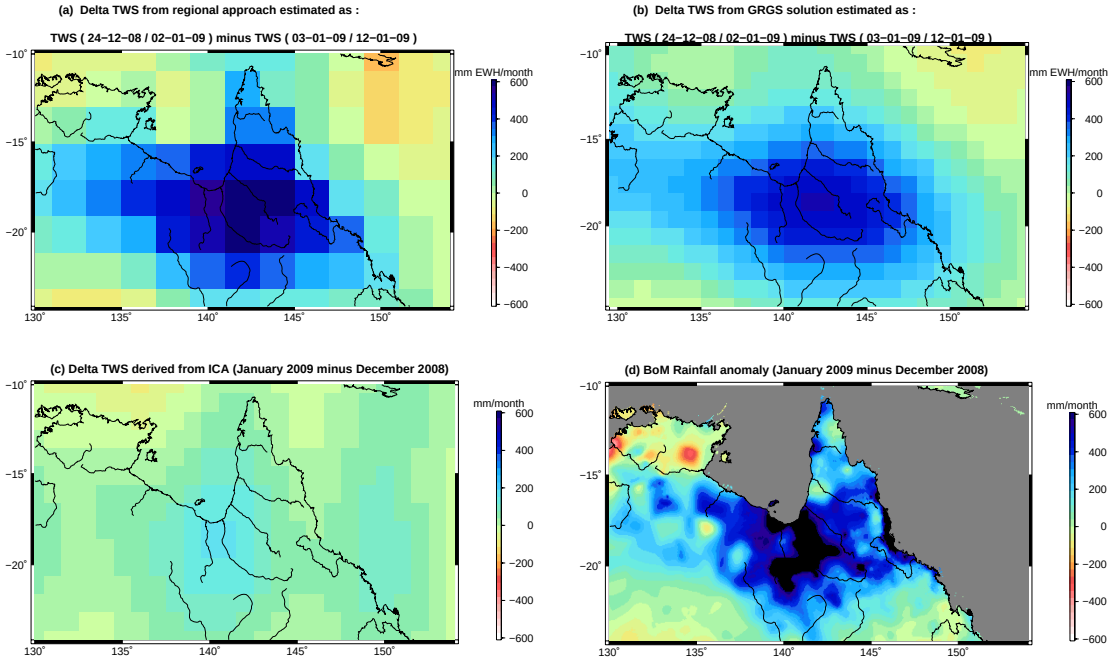

Fig. 12. ΔTWS time series map derived from regional solutions **(a)**, from GRGS RL02 **(b)**, from ICA solutions **(c)** and rainfall anomalies for January 2009 **(d)**. We can notice on January solutions the strong amplitudes in the Gulf of Carpentaria due to the floods caused by the cyclone Charlotte (8 January–12 January 2009).

HESSD
10, 5355–5395, 2013

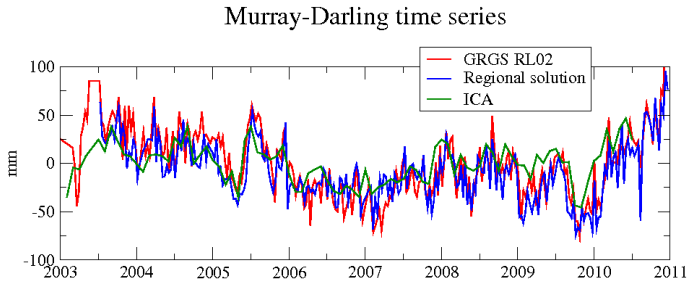

Fig. 13. 10 days and monthly time series of averaged total water storage over the whole Murray–Darling Basin from 2003 to 2011 computed from 10 day GRGS global solutions (red line), 10 day regional solutions (blue line) and monthly ICA 400 km filtered solutions (green line).

HESSD
10, 5355–5395, 2013

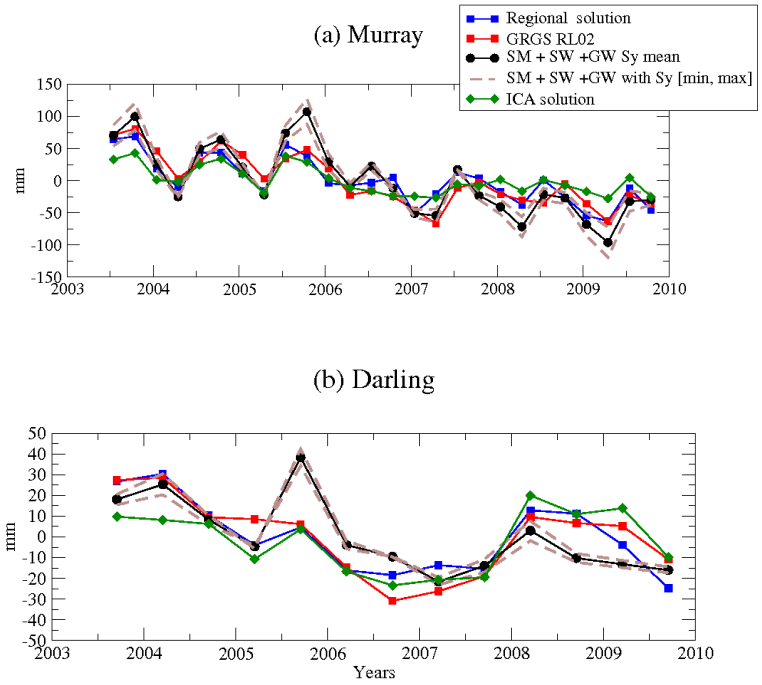

Fig. 14. (a) 3 month averaged time series of TWS over Murray Basin and **(b)** 6 month averaged time series of TWS over Darling basin for 2003–2010. Series are computed from GRACE-based regional solutions (blue line), GRGS RL02 (red line), ICA 400 km filtered solutions (green line) and TWS estimated as groundwater storage + surface water observations + modeled soil moisture (grey lines). Discountionous grey line: Maximum and minimum values of the specific yield are used (values of 0.06 and 0.14); Continiuous grey line: mean value of specific yield is used (0.01).

HESSD
10, 5355–5395, 2013

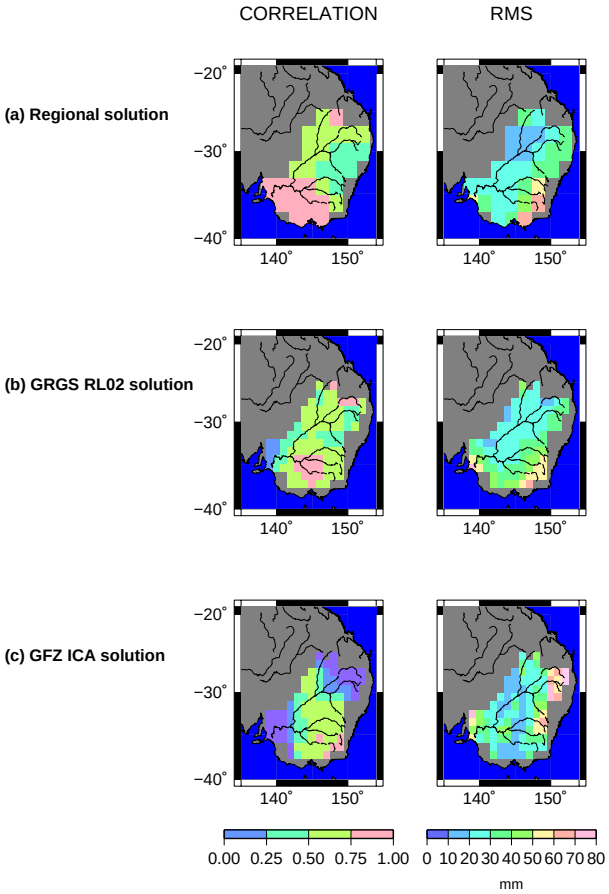

Fig. 15. Spatial correlation (left maps) and RMS (right maps) of differences between TWS (in-situ GW measurements + surface water + modeled soil moisture) and: **(a)** regional solutions, **(b)** GRGS RL02 solutions and **(c)** ICA 400 km filtered solutions.

HESSD
10, 5355–5395, 2013